A TALE OF TWO STORMS: AN INTEGRATED FIELD, REMOTE SENSING, AND MODELING STUDY EXAMINING THE IMPACT OF HURRICANES FRANCES AND JEANNE ON CARBONATE SYSTEMS, BAHAMAS

Stacy L. Reeder and Eugene C. Rankey
Comparative Sedimentology Laboratory and
Center for Southeastern Tropical Advanced Remote Sensing
Rosenstiel School of Marine and Atmospheric Science
University of Miami
Miami, FL 33149
e-mail: sreeder@rsmas.miami.edu

Abstract

Tropical cyclones commonly are cited as being influential, or even dominant, controls on the geomorphologic evolution of carbonate systems, and their influence is highlighted in many interpretations of ancient platforms. A unique opportunity to explore the effects of storms on platform systems occurred when two strong tropical cyclones (Frances and Jeanne) passed directly over the shoals and reefs of the Abacos, northern Bahamas, in 2004. Observations of the influence of these storms coupled with hydrodynamic observations and wave models provide insights into the nature and extent of geomorphologic change that might be related to the passage of such storms.

Comparisons of high resolution (2.4 m pixels) QuickBird remote sensing images and modeling lead to a conclusion that storms have spatially limited effects on the subtidal platform and shoals, and that storms are neither sufficient to alter the system nor necessary for lobate shoals to form. Instead, daily processes (winds, waves, and tides) produce conditions adequate to explain geomorphic features.

The effects of these two storms are not enough to explain the geomorphic evolution of this tidally influenced system. Other studies show that storms had comparable impacts, suggesting that this is not an exceptional case. These observations are consistent with a quantitative wave model showing the distribution of energy across carbonate systems with different geometries. These observations and model results highlight the difficulty of generating grainy ‘storm deposits' of comparable extent to those interpreted in some ancient successions. Collectively, these observations and models question the paradigm of storm influence on shallow-water carbonate platform geomorphology.

Introduction

Tropical cyclones are commonly invoked as significant geomorphic and geologic forces that shape carbonate sedimentary systems (Perkins and Enos, 1968; Ball, 1967; Wanless et al., 1988; Wanless and Tedesco, 1993; Scoffin 1993) due to their powerful forces including excessive wind speeds, increased current velocities, storm surges and a broader higher-energy wave spectrum. In many ancient carbonate successions, thin, but apparently laterally extensive, grainy beds have been interpreted as storm-generated deposits (Aigner, 1982; Aigner, 1985; Jennette and Pryor, 1993; Kreisa, 1981; Kreisa and Bambach, 1982; Seilacher and Aigner, 1981). Additionally, many stratigraphic studies highlight interpretations of 'storm-dominated platforms' and 'storm wave base' (reviews by Ager, 1981; Aigner 1985; Pomar, 2001). At a smaller scale, many lobate features on Holocene platforms were originally described as "spillover lobes," (Ball, 1967) with a morphology interpreted to be driven mainly by storms (Hine, 1977). Nonetheless, although storms frequently traverse carbonate platforms, direct observations of major storm impacts on carbonate platforms are relatively rare (Major et al., 1996). In fact, some studies have illustrated the lack of impact of storms on carbonate systems (Boss and Neumann 1993; Rankey et al., 2004).

The passage of two tropical cyclones (Hurricanes Frances and Jeanne) over the same area on Little Bahama Bank, Bahamas, within one month in September 2004, provided a unique opportunity to examine the impact of strong tropical storms on active Holocene carbonate systems. If storm-generated morphological changes were ever expected to occur, they should be readily apparent after the passage of *two* storms over the same area within a month's time.

The purpose of this paper is to describe the impacts of these storms, explicitly exploring the hypothesis that storms are not a major influence on the geomorphology of the shoals in this region. To further explore the effects of storms, a wave model studies the depths of influence of storm waves on more simplified carbonate bathymetries such as a gentle ramp or a flat, un-rimmed carbonate platform. The results of the modeling suggest that larger storms are not necessarily more influential on the geomorphology of platform top carbonate shoals since the larger waves are more likely to break over the platform edge. The results are important in understanding the fundamental processes involved in shaping the geomorphology of carbonate systems. Additionally, they raise questions regarding the realism of interpretations of widespread storm deposits in analogous systems in the ancient.

Background

Study Area

The study focuses on observations from the northwestern portion of the Abaco Island chain, on the northern edge of Little Bahama Bank. Little Bahama Bank is an isolated carbonate platform bound by the Atlantic Ocean to the north and east, the Straits of Florida to the west, and Northwest Providence Channel to the south. A discontinuous barrier reef is located at the northern shelf break (Figure 1). The western portion of the northern boundary of the study area contains a 5 km-wide breach in the reef complex, through which many open-ocean waves can pass without being effected by the bottom. This area is deeper (~ 10+ m deep) than the adjacent parts of the shelf located behind the reef (~ 6 - 7 m deep), and the sandy bottom includes many areas with symmetrical skeletal sand ripples (~ 0.15 m high, spaced about 0.30 m apart), although large (up to 5 m relief) patch reefs are common. East of this break, the barrier reef is continuous for 10.5 km, and is flanked by a reef apron that extends ~ 1 km onto the platform. The apron is generally ~ 4-5 m deep, and it consists mainly of a skeletal sandy bottom. Between the reef apron and the island system (a distance of ~ 4.5 to 5 km), the sea-bottom consists mostly of peloid-skeletal packstone to grainstone largely stabilized by seagrass, and abundant patch reefs. [In this paper, although these sediments are not rocks, for ease, the Dunham classification based on grain support and mud content is used to describe the modern depositional texture.] Rocky islands formed by Pleistocene eolianite are separated by inlets that focus the tidal flow. Flood and ebb tidal deltas in the area consist of generally lobate forms, convex away from the islands with endpoints near the inlets (Figure 1). The ebb deltas extend up to 2 km from the islands towards the reef, but the flood deltas mostly remain within 1.3 km of the islands. Although the inner portions of these lobes are mainly seagrass-stabilized fine-sand-sized peloid-skeletal packstone with a few small local patch reefs, the main channels are generally hard bottomed (assumed to be Pleistocene bedrock) with growth of hard and soft corals and sponges. Outwards from the inlet center, this hard bottom passes into coarse lag and eventually into a seagrass-stabilized area before reaching the active oolitic shoals, which form the crest of the deltas. Many flood deltas include rock ridges parallel to the island trend, and not all facies are represented in every flood lobe due to the different sizes and shapes. South of the Abaco island chain, the surface of Little Bahama Bank consists largely of peloid-skeletal wackestone to packstone and is stabilized by seagrass.

Oceanographic and Meteorological Setting

The physical setting of the study area dictates the daily oceanographic forces to which it is exposed. The tidal deltas are exposed to the open Atlantic Ocean to the north and are therefore prone to larger swells from this direction than from the shallower bank to the south, although the continuous sections of the barrier reef reduce the impact of these larger swells. Similarly, the islands shield the bank from incoming open-ocean swells, creating a mixed tidally-dominated system that is predominately semidiurnal. The tidal range in the region averages around 1m (cf. Reeder, 2007).

The area is influenced by several winter cold fronts annually. Such events have been documented as a significant cause of erosion in areas such as the northwest coast of Andros Island, Bahamas (Shinn et al., 1969; Rankey and Morgan, 2002). These fronts are accompanied by stronger than average winds from the north and northeast that differ both in direction and in magnitude from the otherwise dominating easterly Trade Winds.

The Abacos are prone to tropical cyclones from June through November. In 2004 alone, two major tropical cyclones passed directly over the study area. On 4 September 2004, Hurricane Frances (Figure 2A) passed through this region as a category 3 storm on the Saffir-Simpson scale (sustained winds of 50 to 58 m/s), decreasing in intensity to a category 2 (sustained winds of 43 to 49 m/s) upon departure (Beven, 2004). Less than a month later, on 25 September, Hurricane Jeanne (Figure 2B) passed through the same area as a strong category 3 storm. These storms did considerable damage to the Bahamian communities in the area, many of which are still struggling to recover.

Observations

An ultra-high-resolution (2.4 m^2 pixel size) QuickBird remote sensing image acquired on 27 November 2003, prior to the passage of these two storms, provides information on pre-storm morphology. For comparison, a second QuickBird image was obtained on 16 March 2005, after the passage of the storms. This data, calibrated by field observations, provide an important foundation for this study; however, differences in boundary conditions for each image acquisition (different atmospheric conditions, time frames, wave climate, tide level, etc.) limited quantitative comparisons between images. Bathymetry derived from satellite data (Stompf et al., 2003) is not accurate enough to measure centimeter-scale changes. Therefore, it cannot be determined if sediment was either eroded from or deposited to the existing system through the available datasets.

What changes resulted from the passage of the two hurricanes?

Comparisons between these two datasets demonstrate very little geomorphic change in the study area. In many areas, the two images appear more-or-less identical (Figure 3), illustrating little to no change. For example, the reef aprons show minimal morphologic change after the passage of the two storms, and the majority of the shelf behind the reef does not illustrate any noticeable change in the remote sensing images. There are, however, some minor modifications to the platform after the storm passage. In the shelf region behind the reef, just seaward of the deltas, a couple of the linear bars and blowouts (Figure 1) experienced some sea-grass removal and slight (<10 m) eastward expansion of the blowouts.

The most pronounced changes in the study area occur in the crests of the tidal deltas (Figure 4) where some sand wave crests migrated ~30-35 m, but none of the crests moved more than 50 m. On the ebb lobes, some shoal crests migrated to the southeast. The largest change in the ebb lobes occurred in the southwestern portion of the area illustrated in Figure 4. In the 2003 image, there is a small (~35 m) seagrass-stabilized area on the shoal (black dashed box in Figure 4, C). In the 2005 image, this small region has been "filled in" with sand. The crest of the northern lobe in the area of the black dashed box of Figure 4, C migrated ~30 m westward, whereas the adjacent crest south west of this one did not move as much. The linear bar (Figure 1) perpendicular to this region also broadened.

The flood deltas showed the most obvious changes over this 2-year period. The sandy extent of some deltas expanded ~30-60 m out onto the platform and ~10-20 m laterally (relative to the central channel). Many of the sand wave crests of the flood deltas followed similar trends to those on the ebb deltas and migrated to the west-southwest. Some of the crests, however, move islandward (solid black box in Figure 4, C), and others move to the east.

These observations indicate that the storms did modify the carbonate platform, at least a little. The crests of some sand waves migrated 30+ meters. Such modifications to the shoals may be due to the passage of the two storms. With the direction of approach of both Hurricane Frances and Hurricane Jeanne, the strongest winds would have come from the northeast, which may account for the southwestern migration patterns. However, storms should not be considered the only possible explanation for these morphologic adjustments. Sandwaves can migrate ~4 m in a month under fair-weather conditions in a tidal channel (Gonzalez and Eberli, 1997). The observed sand wave migration rate of 20 m/year at the tidal deltas is lower than this documented rate, but these rates are highly dependent on the tidal velocity. On the tidal deltas, the current velocities range between 0.24 and 0.30 m/s, so the rates of sand wave migration may be much smaller here.

The lobes themselves remained generally stationary, and modifications occurred mainly in sand wave crests. Overall, on the tidal deltas, there was no major reorganization of the shoal geometries (e.g., no new ‘spillover lobes’). Only minor changes are apparent, such as removal of small patches of seagrass (Figure 5, red boxes), smearing of sand waves on shoal crests, and slight expansion of the shoal by deposition of a thin layer of sand ~60 m outward in some areas (Figure 5, orange and green boxes). In the big picture of the carbonate platform, these are small perturbations, and, although it is possible that such small perturbations may be further amplified by daily processes, this does not appear to occur here. Observations (in summer 2005) of sand waves re-forming and sea grass re-establishing suggest that the system was returning to its pre-storm state.

Field observations led to further questions about the influence of storms on the platform. No major discernable sediment erosion or deposition was observed in the field.

Many of the areas of “shoal widening” on the remote sensing images proved to be a thin layer of sediment that transported off the shoal crest onto adjacent grassy areas rather than a large addition to the lobe, and these areas were beginning to stabilize by seagrass in summer 2005. These observations indicate that the daily tides, winds and waves of the region are restoring the system from the minor perturbations brought about by storms. Although storms may modify the system in the short-term, it appears unlikely that such perturbations will be preserved.

Modeling Storm Waves: What might they do?

The field and remote sensing observations suggest relatively little impact of the storms on this carbonate system. In the context of the often assumed geological importance of storms, this result is not trivial, given the apparent strength of the storms, and the fact that two passed over the area in a short time period. To further investigate the potential influence of storms, a simple wave model was used to explore the forces that might be exerted by storm waves on a carbonate platform.

The model consists of two main parts: a wave prediction module and a wave transformation module. The wave prediction module computes the deep water significant wave height (the average wave height of the highest 1/3 of the measured waves in a location) and peak wave period for a given wind speed. As the waves approach shallow water, the wave transformation module of the model computes the adjusted significant wave heights and the bottom orbital velocities produced by these waves. Breaker criterion are used to calculate the maximum height of a wave before it will break and are used to determine the depth at which the wave will break. Once the wave breaks, the heights and orbital velocities are set to zero, terminating the propagation of the wave as well as any sediment transport that may have been initiated.

The wave model was run for two different bathymetrical configurations (Figure 6). The simplest bathymetry was a ramp sloping at an angle of 0.3º from horizontal, spanning 10 km (Figure 6, A). The second bathymetrical configuration that was studied simulated a simplified flat-topped platform. In this case, a 5 m deep shelf dropped steeply (14°) to deep water at the shelf margin, mimicking some Bahamian platforms (Figure 6, B).

Deep water wave model:

Initially, the deep-water wave heights (H_o) are calculated for a given wind speed measured 10 m above sea level (u_{10}) using the deep water fetch-limited wave equations (e.g., Komar, 1976)

$$\frac{gH_0}{u_*^2} = 1.6 \cdot 10^{-3} \left(\frac{gF}{u_*^2} \right)^{1/2},$$

where g is the acceleration due to gravity (~9.81 m/s^2), F is the fetch, and u_* is the wind stress factor. Given a known u_{10}, the wind stress factor is

$$u_* = 0.71 u_{10}^{1.23}.$$

Wind waves are initially dependant on the time the wind has been blowing (duration) as well as the distance over which it has blown (fetch). After a certain period of time, the waves are no longer time dependent and become fetch-limited. To ensure that the waves are past the limit for a duration limited sea state and that the fetch limited equation given above is adequate for calculating the wave heights, the model computes this time limit (t_d) using

$$\frac{t_d g}{u_*} = 68.8 \left(\frac{gF}{u_*} \right)^{2/3}.$$

The model then assumes the wind has been blowing steady longer than this limit to the duration limited sea state. The model then generates waves from a fetch of 16 km (based on an assumption of a 10-mile scale for daily land or sea breezes). Model runs with other fetch values (25 and 50 km) yielded similar results to the 16 km fetch, except the larger waves produced by a longer fetch broke in deeper water such as at the platform margin, limiting the waves that pass over a platform. The calculations with the 16 km fetch produced waves that propagated over the platform rather than breaking at the platform edge, for most wind speeds.

The model computes the peak wave period for the given wind conditions using

$$\frac{gT_p}{u_*} = 0.286 \left(\frac{gF}{u_*^2} \right)^{1/3}.$$

The effects of four different wind conditions representing the daily trade winds, winter North Easters, tropical storm winds, and hurricane (Category 1) strength winds are explored with the model. Table 2-1 gives the results of the deep water wave prediction module.

Wave transformation and breaking:

Waves generated in deeper water can propagate towards the coast (carbonate ramp) or across a platform. As waves enter relatively shallow water, the waves shoal, indicating that the wave height increases, the wave length (L) decreases, and steepness (ratio of wave height to wave length) increases. The wave height (H) at a given depth (h) is computed using the equations for wave shoaling:

$$H = H_0 k_s$$

$$k_s = \frac{H}{H_0} = \left(\frac{1}{2n} \frac{c_O}{c} \right)^{1/2},$$

where k_s is the shoaling coefficient (relates the deep water wave height to the wave height at a given water depth, h), c is the wave phase velocity (the speed of individual waves), c_o is the deep-water wave phase velocity $\left(c_O = \frac{g}{2\pi f} \right)$, $f = \frac{1}{T_p}$, and n is defined as:

$$n = \frac{1}{2}\left[1 + \frac{2kh}{\sinh(2kh)} \right],$$

where h is the water depth and k is the wave number. For simplicity, the model assumes shore-perpendicular waves and shore-parallel depth contours; therefore, wave refraction can be neglected.

Storm surges were incorporated by adding the average surge estimated by the Tropical Prediction Center/ National Hurricane Center for each type of storm (Table 2-2) to the bathymetrical profile (in the above equations, substitute (h + Surge) for h), but the current velocities produced by a storm surge were not modeled. These currents, however, may be important to the overall impact of the storm and cause down-slope transport during surge retraction.

Since the point of the model is to explore the effects of storm waves on a sedimentary system, the model computes the bottom orbital velocities for the shoaled waves through linear wave theory. For each point along the bathymetrical profile, the bottom orbital velocity (u) is computed by

$$u = \frac{\pi H}{T_p \sinh\left(\frac{2\pi h}{L}\right)}.$$

To determine the effects of the waves on the sediments, the bottom orbital velocity was compared to the threshold velocity (u_t) for entrainment of sediment of which 50% of the grains have a diameter smaller than d_{50}.

$$u_t = \sqrt{8g\left(\frac{\rho_s}{\rho_w} - 1\right)d_{50}},$$

where ρ_s and ρ_w are the densities of the sediment and water, respectively. In the model, the threshold velocity for sediment entrainment of sediments of 0.5 mm in diameter (approximately the average size of the Abaco tidal delta sands) with an average density of 2.75 g/cm^3 (Incze, 1998) is 0.26 m/s. This velocity, however, is calculated for bare sand. If the bottom contains seagrass or is partially cohesive due to algae or cementation, the threshold velocity could be much higher. The depths at which sediment transport begins are therefore most likely smaller than those calculated with $u_t = 0.26$ m/s.

As the wave steepness increases through shoaling, it can reach a point where the wave breaks. To determine the wave height at the point where it breaks as well as the depth of the water when the wave breaks, the model includes a breaker criterion (Kaminsky and Kraus, 1993). Once a wave exceeds the breaking condition

$$H_b = \gamma_b h_b,$$
$$\gamma_b = 1.20\xi^{0.27},$$
$$\xi = \frac{S}{\sqrt{\frac{H_O}{L_O}}},$$

(H_b is the critical wave height at which point the wave breaks, $L_o = \frac{gT_p^2}{2\pi}$ is the deep water wave length and S is the bottom slope), the wave breaks, the wave height is set to 0.00 m, the bottom orbital velocity is set to 0.0 m/s, and the waves do not regenerate in this model.

Application to a carbonate ramp:

To investigate the physical potential of laterally extensive storm deposits that have been interpreted in the stratigraphic record, the wave model was first run for a gently sloping ramp (Figure 6, A). Table 2-3 and Figure 7 provide the results of these calculations.

For the tropical storms, the waves can break in 3.90 m of water, while the category 1 hurricane can produce breaking waves in 8.21 m of water depth which move the sediments beginning in depths of 12.37 m prior to breaking. For these stronger storms in the real world, the waves lose energy to white capping and non-linear interactions, so the cases illustrated in Figure 7 represent waves larger than would actually occur. The depths of influence, therefore, are also larger than should be expected. Overall, with the modeled waves from the peak of the wave frequency spectrum, the maximum depth of impact on a ramp occurs during a Category 1 Hurricane. In these conditions, the waves can begin to move bare sediments in 12.37 m of water (these depths include the surge values, so this depth corresponds to a depth of 10.87 m below mean sea level). These results are consistent with the results of detailed studies of wave impact on exposed coasts which indicate that significant sediment transport due to waves will not occur below 20 m of water depth (cf. Dietz and Fairbridge, 1968; Duane, 1976; Gordon and Roy, 1977). A similar study on a coast with low wave energy (Sapelo Island, Georgia; Coastal Engineering Research Center, 1984) further limited this depth to less than 10 m on coasts exposed to lower wave energy (~ 0.25 m annually averaged significant wave height), and the model results are fairly consistent with these results, as well.

This data illustrates the difficulty of storm-generated waves impacting broad expanses of ramps, given the model assumptions. It appears that in shallower areas (e.g., less than 5 m), such wind-generated waves could, however, have an impact. At these depths, bottom effects cause the waves to disperse their energy through sediment transport and eventual breaking.

Application to a carbonate platform:

To investigate the effects of storm-waves on a platform, the model computed the wave heights, bottom orbital velocities, and breaking limits for a simple, un-rimmed carbonate platform (Figure 6, B). The platform configuration does not include shoals such as the tidal deltas of the Northern Abacos, but understanding the potential influence of storm waves on a flat platform is useful in understanding the forces that could possibly impact such a shoal system. The results of the wave model as applied to a simplified platform are summarized in Table 2-4.

The case of the platform margin (Figure 8) provides insights on how a more complex bathymetry might be impacted by storm waves. Although sediment transport on the platform top can be initiated from waves produced by 18 m/s storm winds, the bottom orbital velocities remain below 1.2 m/s for even the strongest of storms on the platform. From the results presented here (Figure 8, Table 2-4), the most influential storm would be similar to the winter storm (12 m/s winds). The waves produced from winds around 12 m/s (under the assumed duration and fetch) do not produce bottom orbital velocities large enough to initiate sediment transport on the platform. Although the maximum orbital velocities are larger than the threshold velocity, the depth of initiation of motion is shallower than the platform depth, so the sediment does not move along the platform (the 12 m/s winds initiate sediment motion at 4.1 m depth, but the platform depth is 5.5 m with the surge set up for this storm). Instead, motion is initialized at the shallower-end of the bathymetrical profile, which could indicate the location of a carbonate shoal body (Figure 6, B). For winds stronger than 18 m/s, the wave break at the edge of the platform, so the platform sediments will not be affected by these waves. There remains a small window of storm intensities that can influence the platform interior and hence, the carbonate shoal bodies.

Model assumptions and limitations:

This simple model fails to show the post-breakage effects. As waves enter the platform over the shelf margin, they are modified by bottom effects. The larger swells break at the platform edge upon hitting shallow water, since the maximum wave that can occur is a fraction of the water depth. The waves that break can re-form, but due to the short fetch and shallow depths of the region between the reefs and the islands in the study area, these regenerated waves can not grow to the size and force of the original swells that broke at the platform edge. These dynamics introduce an interesting paradox. Although larger storms produce bigger waves offshore, a category 4 or 5 storm may lead to less wave-influenced transport on the platform than a less intense storm such as a winter cold front. The reefs, however, will likely feel more of an impact from these large storms. The relationship between storm strength and storm impact to the carbonate system, can therefore vary spatially across a platform.

Another limitation to this wave model is that it only considers the peak wave period of the wind-wave spectrum. Although this wave may break, there are some wave height and period combinations that would penetrate into shallower waters, either on the ramp or along the platform. Although the model may indicate that the waves have broken on the reef, it is possible that some waves produced by a particular windspeed may yield sediment transport beyond the point of breaking for the peak period waves.

Furthermore, wave generation by wind on the platform was not explored in this simple wave model. As a strong wind traverses a carbonate platform, it will produce fetch and duration-limited wind-generated waves. These waves will not have to pass over a steep slope, so they may be able to produce more sediment transport on the platform than the waves coming from the deep ocean.

Finally, the estimated values of wave heights, bottom orbital velocities, and depths of initiation of motion or breaking from the model represent the maximum values for several reasons. In the case of a reef-rimmed platform such as the Abaco tidal delta region, the majority of the waves would break over the reef, so the conditions depicted in the flat-topped platform model correspond to the highest waves and orbital velocities on the reef-rimmed platform.

Storm forces versus day-to-day processes

Storms have an effect on sediment distribution. The modeling illustrates how tropical cyclones can yield large enough bottom orbital velocities to move sediment, and observations after hurricanes Frances and Jeanne illustrated limited redistribution of sediment, with the most pronounced changes occurring in the flood tidal delta lobes. However, the question remains as to how much effect the storms have on shaping geomorphic bodies and, eventually, the sedimentary record. Although they may impact geomorphology slightly in the short term, are they enough to counter-act the daily processes?

To quantify the daily forces that act on the platform in the study area, waves and currents were measured during the summer and fall of 2005. Two bottom-mounted, pressure-sensitive wave gauges (see Figure 1 for location) measured the sea state for August and September. One wave gauge was kept stationary throughout the sampling time at a location between an ebb lobe and the barrier reef (blue dot in Figure 1) while the second gauge spent 2 weeks inside the ebb lobe (light blue dot in Figure 1) and was then transferred to the deeper water near the break in the barrier reef (green dot in Figure 1). Simultaneously, a bottom-mounted Acoustic Doppler Current Profiler (ADCP) was placed for one month at a time in two different tidal inlets (Figure 1, located at ADCP1 in August and ADCP2 in September), and measured the 3-dimensional velocity profile in 4 minute intervals, averaging over 3 minutes. This data was compared to atmospheric conditions monitored at the nearest National Oceanographic and Atmospheric Administration (NOAA) buoy, located at Settlement Point on Grand Bahama Island, ~105 km to the southeast (Figure 9). Although this data may not represent the exact atmospheric conditions of the study area, the winds measured at the buoy and the waves measured at the study site appear to correspond nicely.

The storm of 24-27 August (Figure 9, red dashed box) is Hurricane Katrina, which passed ~160 km south of the study area. In the Abacos, winds were from the north as the storm first approached, then from the east as it passed south of the area. The waves produced by this storm persisted for two days, but significant wave heights remained smaller than one meter (Figure 10). The bottom currents were only slightly modified from the rest of the tidal cycle's magnitudes. From the simplified storm wave calculations described previously, this corresponds to conditions analogous to the 12 m/s winds, which may produce waves that could move sediment in waters shallower than 4.8 m. Therefore, the combination of the currents and waves produced by this storm could have impacted the tidal deltas, albeit for a short time period, and changed them somewhat.

In comparison, the daily bottom tidal currents of the tidal deltas approach and can exceed 1 m/s in some areas (Figure 10), much greater than the threshold velocity of sediment entrainment of the average diameter (0.5 mm) for ooids found in the tidal delta region (0.26 m/s). Although the velocities produced during a storm may be greater than these tidal velocities, they are short-lived. In contrast, tides move in and out, day after day, re-applying the same forces to the system. Therefore, although sediment may be transported and re-deposited during storms and periods of higher-than-average velocities, the duration of storms may not be enough for significant morphological adjustments. Likewise, based on our continuing observations (described above) it is possible that the daily forces may be enough to re-adjust the system back to its previous morphologic state.

Discussion

Why only subtle changes?

Strong storms are destructive. Many lives have been lost to tropical cyclones (e.g., the Galveston storm of 1900), and they can cause extensive property damage (e.g., Hurricane Andrew, 1992; Hurricane Katrina, 2005). In regions containing sandy barrier islands and beaches, a single storm can cause considerable damage along the shore due to storm surges and waves (Hill et al., 2004; Keen et al., 2004; Stone and Orford, 2004; Stone and Wang, 2004). However, impacts on tidally influenced subtidal seascapes such as the oolitic tidal deltas and shelf margin of the Northern Abacos appear much less pronounced.

The remote sensing images clearly demonstrate that although there were no major lasting geomorphic changes (e.g., new ‘spillover lobes,’ or extensive movement of sands) as a result of passage of these tropical cyclones, there are indeed some geographically limited changes to this system. In the study area, between the 2003 and 2005 image acquisitions, crests of sand waves appear to have moved, and sand was transported off the shoal crest over adjacent grassy areas. If these changes were not due to day-to-day processes (the observations do not permit this possibility to be eliminated), these small apparent changes imply that either:

a) changes were simply too small to observe on the ultra-high resolution remote sensing data, or there simply were no changes. This could be due to the presence of a storm surge, which diminishes the impact of the storm waves on the platform by increasing the water depth. This result indicates that, although storms may be powerful, they are not the most important forces shaping geomorphology in this and analogous depositional systems.

b) there were alterations due to storms, but they returned to their original state after the storms and before acquisition of the second image and field observations. If this situation is valid, it would emphasize the role of daily processes in shaping the overall morphology of the shelf.

Tropical cyclones are indeed powerful; they produce large waves and storm surges, both of which can generate strong currents. The models (Figures 7, 8) illustrate that although not all storms (from winter storms to strong cyclones) produce waves strong enough to impact the bottom in all areas, they appear to have important roles in two regions. The first area is at the shoreline. In all cases, energy is expended on the shoreline due to breaking; this energy would be greater than that due to the daily (non-storm) waves. In these areas, more pronounced changes are expected. In the Abacos study area, many of the islands are rocky, and do not have sandy beaches, which may explain the lack of change at the shoreline. The second important area is the 'outer shelf' between the reef and the shore. Some, but not all, storms produce waves large enough to be impacted by the bottom in this area. These deeper areas (between 5 and 12 m deep) are beyond the penetration depths of daily waves (Figure 8A). Tide and wind generated currents, which are weaker in these less-restricted regions, become much stronger in the presence of high winds and storm surges. Thus, in these areas, some sediment may have been suspended and transported.

Another possible interpretation for the lack of significant change is that the geomorphic elements formed in response to storms earlier in the geologic history of the region, and are now in 'equilibrium' with such high-energy conditions. Many tropical cyclones and storm fronts pass through this area (Landsea et al. 2003) and the tidal delta region of the Abacos must have been subjected to a very large quantity of storms ranging from tropical cyclones to winter cold fronts throughout its history. However, this hypothesis is unlikely for several reasons. Visual observations at the study site revealed active sediment transport with the daily tidal cycles. These observations suggest that the forms are not relict, being modified only by high energy storm events, but they are changing daily. Also, if they were to be formed by storms, as "spillover lobes," it would be difficult to obtain such well-defined lobes on both sides of the islands. The storm patterns as discussed previously would most likely lead to larger "flood" lobes than "ebb" lobes, whereas the observations illustrate the opposite relation. Therefore, it is unlikely that these geomorphic bodies were formed by storms, and it is more likely that they are the result of daily forces.

Perspectives and Limitations

Based on his modeling study of wave-dominated shorelines, Storms (2003) wrote that "…the shallow-marine stratigraphic record is built predominantly by high magnitude–low frequency processes rather than low magnitude–high frequency processes." Similarly, Quiquerez, et al. (2004) wrote that "…observations therefore suggest that… storm events and reworking of sediments contribute significantly to the sedimentary record on ancient continental shelves at long time scales…." Wanless et al. (1988) summarized 25 years of research saying that "a large body of literature has suggested that catastrophic events are a dominant influence on sedimentation in shallow-marine carbonate environments." These types of statements form the basis of interpretations of storm deposits of great lateral continuity in ancient successions, such as the beds interpreted by Jennette and Pryor (1993), to be continuous across an area greater than their 32 x 35 km study area.

In stark contrast, the observational and modeling results of this study illustrate that storms are neither sufficient nor necessary to explain geomorphic features and subtle changes in the Abacos carbonate system. Similarly, evidence for aerially extensive tempestite deposits, such as those commonly attributed to storms (Aigner, 1985), remains to be observed in many Holocene carbonate systems (Gagan et al., 1988 is a notable exception; cf. Wanless et al., 1988), although it is not for lack of trying. For example, Robert Ginsburg (pers. comm., 2006) related how he had an associate examine the shelf off Key Biscayne, FL, immediately following the passage of a Category 5 storm, Hurricane Andrew, directly over the area. The person found merely a cm-thick layer of mud in some places. How might this apparent paradox be reconciled?

The answer, of course, is that storms can have an impact. Carbonate systems are heterogeneous, and interpretations of the dominance or irrelevance of storms cannot be universally applied. Subsequently, perhaps it is better to ask, in what settings might we expect to find the effects of storms to occur?

Similar to siliciclastic shorelines, some carbonate systems are wave-dominated whereas others are controlled primarily by tides. In wave-dominated systems such as the east coast of the United States, it is possible that the added velocities from the storm surge and the increased wave energy of the storm waves may produce greater forces on the carbonate system than those experienced daily. These may drastically affect the system.

Likewise, it is possible that storm surges have an impact on parts of the geomorphic system. Although the models included the increased water depths that would be produced by surge, they did not explicitly include the currents that would be generated by similar storm surges. These could have an effect on the transport of sediment on- or off-shore, but this was not apparent in the shallow areas considered by this study.

In contrast, the modeling of this study highlights elevated velocities on the platform edge and shoals, yet there are relatively few changes in these regions. The measured tidal velocities at the sediment-water interface (Figures 9, 10) in these deltas are not obviously modified by the passage of the storms, even in the presence of significantly larger storm waves (Figures 9, 10). Thus, although the passage of storms may slightly modify velocity patterns, the daily tidal velocities are of a strong enough magnitude to not be affected by these minor perturbations. It may be that features shaped by tidal flows (tidal deltas and sandy shoals) are less susceptible to changes due to elevated velocities brought about by storm surges or storm waves (cf. Rankey et al., 2006). Similarly, the reefs include rigid frameworks that face tides and waves on a daily basis and appear to have been sturdy enough to not be damaged notably by the storms.

Conclusions

Interpretations of storms and hurricanes are implicitly tied to the concepts of wave base and storm wave base (Gulliver 1899; Fenneman, 1902; see review in Dietz, 1963). The latter is generally taken to be “the greatest depth to which wave action ceases to stir sediments” (Dietz, 1963, p. 973) and is often cited as a sedimentologically important water depth, even if its value is never quite known. Its importance has extended to concepts of shelf profiles, (the classic ‘undaform’ of Rich (1951) and the ‘wave-base razor' of Cross and Lessenger (1997)) and even so far as to be used to estimate amplitudes of sea-level change (Immenhauser and Scott, 2002).

The observations and modeling of this study illustrate that storms are neither sufficient nor necessary to shape the geomorphic patterns observed in this shelf margin system. Although it is likely that tide-influenced and wave-influenced systems respond to storms differently, it still remains that there is precious little direct observational data providing examples of the impact of storms of an extent comparable to those interpreted from the geologic record. This work highlights the need to understand basic physical processes behind sedimentation in carbonate systems and integrate this knowledge to develop new interpretations of ancient successions.

References

Aigner, T. (1982) Calcareous tempestites: Storm-dominated stratification. in Upper Muschelkalk limestones (Middle Trias. SW-Germany). In: Einsele, G., and Seilacher, A., eds. *Cyclic and Event Stratification*, Springer-Verlag, Berlin, p. 180–198.

Aigner, T. (1985) Storm depositional systems: Dynamic stratigraphy in modern and ancient shallow-marine sequences: Berlin, Springer, 174 p.

Ager, D.V. (1981) The Nature of the Stratigraphic Record [2nd ed.]: London, Macmillan Press, 122 p.

Ball, M.M. (1967) Carbonate sand bodies of Florida and the Bahamas. *J. Sed. Petrol.*, **37**, 556–591.

Beven, J.L. (2004) Tropical Cyclone Report: Hurricane Frances: 25 August – 8 September. http://www.nhc.noaa.gov/2004frances.shtml.

Boss, S.K., and Neumann, A.C. (1993) Impacts of Hurricane Andrew on carbonate platform environments, northern Great Bahama Bank. *Geology*, **21,** 897-900.

Coastal Engineering Research Center (1984). Chapter 4: Littoral processes, *Shore Protection Manual*, Vicksburg, MS, **1**, 214 pp.

Cross, T.A. and Lessenger, M.A. (1997) Correlation strategies for clastic wedges. In: Coalson, E.B., Osmond, J.C., and Williams, E.T., eds. *Innovative applications of petroleum technology in the Rocky Mountain Area: Rocky Mountain Association of Geologists*, Denver, CO, 183-203.

Dietz, R.S. (1963) Wave-base, marine profile of equilibrium, and wave-built terraces: A critical appraisal. *Geol. Soc. Am. Bull.*, **74**, 971-990.

Dietz, R.S. and Fairbridge, R.W. (1968) Wave base. In: *The Encyclopedia of Geomorphology* (Ed. R.W. Fairbridge), Reinhold, New York, 1224-1228.

Duane, D.B. (1976) Sedimentation and coastal engineering: Beaches and harbors. In: *Marine Sediment Transport and Environmental Management* (Eds. D.J. Stanley and D.J.P. Swift), Wiley, New York, 493-517.

Fenneman, N.M. (1902) Development of a profile of equilibrium of the subaqueous shore terrace. *Jour. Geol.*, **10**, 31.

Gagan, M.K., Johnson, D.P., Carter, R.M., 1988. The cyclone Winifred storm bed, Central Great Barrier Reef, Australia. *Journal of Sedimentary Petrology*, **58**, 845-856.

Gonzalez, R. and Eberli, G.P. (1997) Sediment transport and bedforms in a carbonate tidal inlet; Lee Stocking Island, Exumas, Bahamas. *Sedimentology*, **44**, 1015-1030.

Gordon, A.D. and Roy, P.S. (1977) Sand movements in Newcastle Bight. *Proceedings of the 3rd Australian Conference on Coastal and Ocean Engineering*, Melbourne, Australia, 64-69.

Gulliver, F. (1899) Shoreline topography. *Am. Acad. Art and Sci. Proc*., **34**, 151-258.

Hill, H.W., Kelley, J.T., Belknap, D.F. and Dickson, S.M. (2004) The effects of storms and storm-generated currents on sand beaches in Southern Maine, USA. *Marine Geology*, **210**, 149–168.

Hine, A.C. (1977) Lily Bank, Bahamas: History of an active oolite sand shoal. *J. Sed. Res.*, **47**, 1554-1581.

Immenhauser, A. and Scott, R.W., 2002. An estimate of Albian sea-level amplitudes and its implications for the duration of stratigraphic hiatuses. *Sedimentary Geology/ ExpresSed*, **152**, 19-28.

Incze, M.L. (1998) Petrophysical properties of shallow-water carbonates in modern depositional and shallow sub-surface environments. PhD dissertation, University of Miami, 405 p.

Jennette, D.C., **and Pryor, W.A.** (1993) Cyclic alteration of proximal and distal storm facies; Kope and Fairview formations (Upper Ordovician), Ohio and Kentucky. *J. Sed. Petr.*, **63**, 183 - 203.

Kamansky, G., **and N.C. Kraus** (1993) Evaluation of depth-limited wave breaking criteria. *Waves '93, American Society of Civil Engineers*, 180-193.

Keen, T.R., Bentley, S.J., Vaughan, W.C. and Blain, C.A. (2004) The generation and preservation of multiple hurricane beds in the northern Gulf of Mexico. *Marine Geology*, **210**, 79–105.

Komar, P. D. (1976) Beach processes and sedimentation, Prentice-Hall Inc.

Kreisa, R.D. (1981) Storm-generated sedimentary structures in subtidal marine facies with examples from the Middle and Upper Ordovician of southeastern Virginia. *J. Sed. Petr.*, **51**, 823-848.

Kreisa R.D., and Bambach R.K. (1982). The role of storm processes in generating shell beds in Paleozoic shelf environments. In: Einsele, G., and Seilacher, A., eds. *Cyclic and Event Stratification*, Springer-Verlag, Berlin, p. 200–207.

Landsea, C.W., Anderson, C.,Charles, N., Clark, G., Dunion, J., Fernandez-Partagas, J., Hungerford, P., Neumann, C., Zimmer, M. (2003) The Atlantic Hurricane Database Reanalysis Project – Documentation for 1851-1910 alterations and additions to the HURDAT Database. *Hurricanes and Typhoons: Past, Present, and Future*, R.J. Murnane and K.B. Liu, eds., Columbia University Press, 2004. 178 – 221.

Major, R.P., Bebout, D.G., and **Harris, P.M.** (1996) Recent evolution of a Bahamian ooid shoal: Effects of Hurricane Andrew. *Geol. Soc. Am. Bull.*, **108**, 168-180.

Perkins, R.D., and **Enos, P.** (1968) Hurricane Betsy in the Florida-Bahama area; geologic effects and comparison with Hurricane Donna. *Jour. Geol*, **76**, 710-717.

Pomar, L. (2001) Types of carbonate platforms: a genetic approach. *Basin Research*, **13,** 313–334.

Quiquerez, A. Allemand, P., Dromart, G., and **J-P. Garcia**. (2004) Impact of storms on mixed carbonate and siliciclastic shelves: insights from combined diffusive and fluid-flow transport stratigraphic forward model. *Basin Research*, **16**, 4-431.

Rankey, E.C., Riegl, B. and Steffen, K. (2006), Form and function in a tidally dominated ooid shoal, Bahamas. Sedimentology, **53**, 1191-1210.

Rankey, E.C., Enos, P. Steffen, K., and Druke, D. (2004) Lack of impact of Hurricane Michelle on tidal flats, Andros Island, Bahamas: Integrated remote sensing and field observations. *J. Sed. Res.*, **74**, 654-661.

Rankey, E.C., and **Morgan, J.J.** (2002) Quantified rates of geomorphic change on a modern carbonate tidal flat, Bahamas. *Geology*, **30,** 583-586.

Reeder, S.L. (2007) Comparative morphology and dynamics of Holocene carbonate systems, northwestern Abaco Islands, Bahamas. Unpublished doctoral dissertation, University of Miami, Coral Gables, Florida, USA.

Rich, J.L. (1951) Three critical environments of deposition and criteria for recognition of rocks deposited in each of them. *Geol. Soc. Am. Bull.*, **62**, 1-20.

Shinn, E.A., Lloyd, R.M., and **Ginsburg, R.N.** (1969) Anatomy of a modern carbonate tidal-flat, Andros Island, Bahamas. *J. Sed. Pet.*, **39**, 1202-1228.

Scoffin, T.P. (1993) The geological effects of hurricanes on coral reefs and the interpretation of storm deposits. *Coral Reefs*, **12**, 203-221.

Seilacher, A., and Aigner, T. (1991) Storm deposition at the bed, facies, and basin scale: The geological perspective. In: Einsele G., Ricken W., and Seilacher A., eds. *Cycles and Events in Stratigraphy*, Springer-Verlag, Berlin, p. 249-268.

Stone, G.W., and **Orford, J.D.** (2004) Storms and their significance in coastal morpho-sedimentary dynamics, *Marine Geology*, **210**, 1-5.

Storms, J.E.A. (2003) Event-based stratigraphic simulation of wave-dominated shallow-marine environments: *Marine Geol.*, **199**, 83-100.

Stumpf, R.P., Holderied, K., and Sinclair, M. (2003) Determination of water depth with high-resolution satellite imagery over variable bottom types. *Limnology and Oceanography*, **48**, 547-556.

Wanless, H.R., Tyrrell, K.M., Tedesco, L.P., and **Dravis, J.J.** (1988) Tidal-flat sedimentation from Hurricane Kate, Caicos Platform, British West Indies: *J. Sed. Pet.*, **58,** 724-738.

Wanless, H.R., and **Tedesco, L.P.** (1993) Comparison of oolitic sand bodies generated by tidal vs. wind-wave agitation. In: *Mississippian oolites and modern analogs* (Eds B.D. Keith and C.W. Zuppmann) *AAPG Studies in Geology*, **35**, 199-225.

Figures:

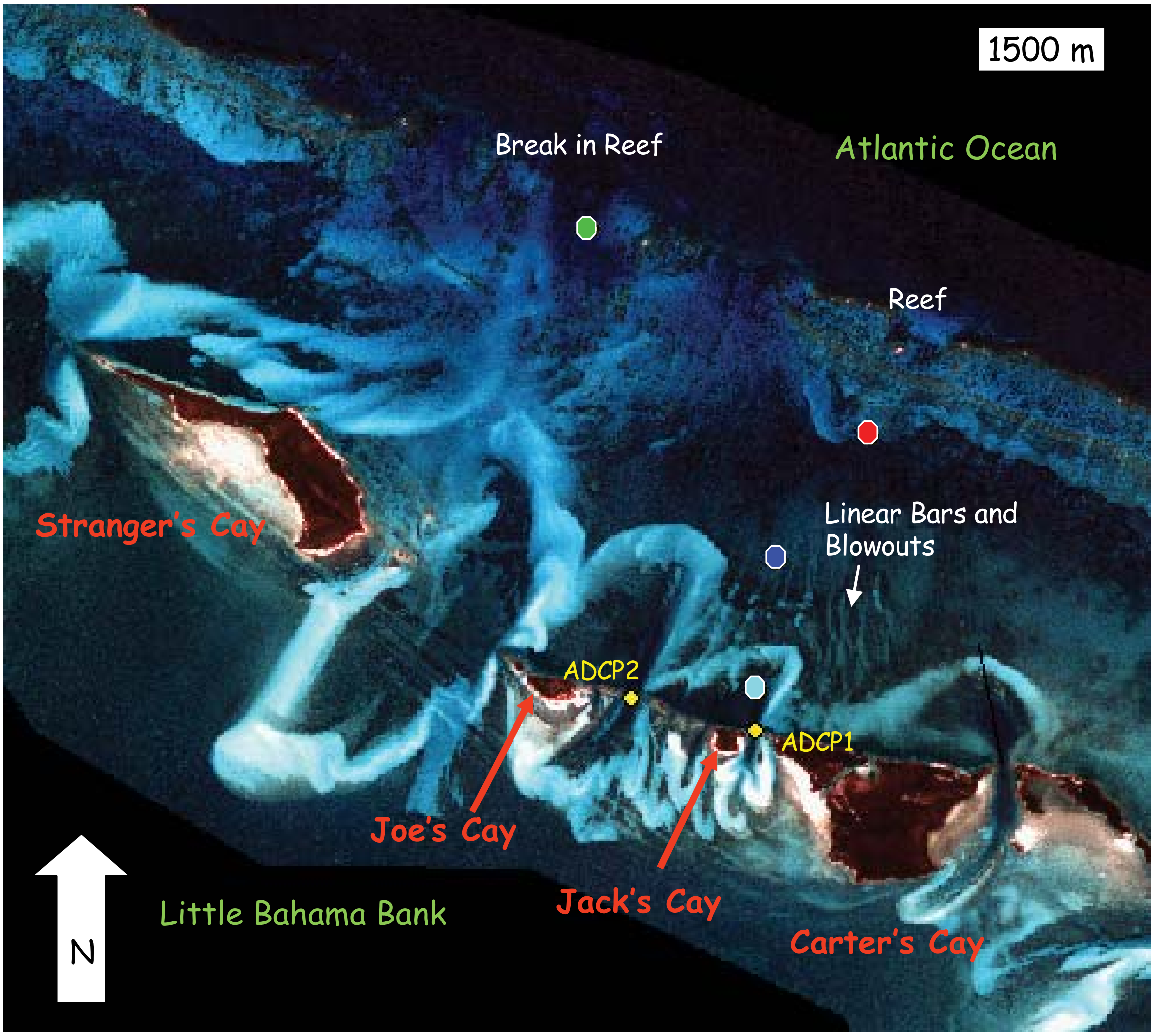

Figure 1: QuickBird image of the region of interest in the Northern Abacos, Bahamas. QuickBird satellite image courtesy: DigitalGlobe. The yellow dots indicate the locations of the bottom mounted ADCPs ("ADCP1" in August and "ADCP2" in September). The green, red, dark blue, and light blue dots indicate the locations of the Dobie wave gauges. There was one at the blue dot during the entire sampling period for calibration purposes, and the other rotated through the other three locations to indicate differences in the wave field during this time period.

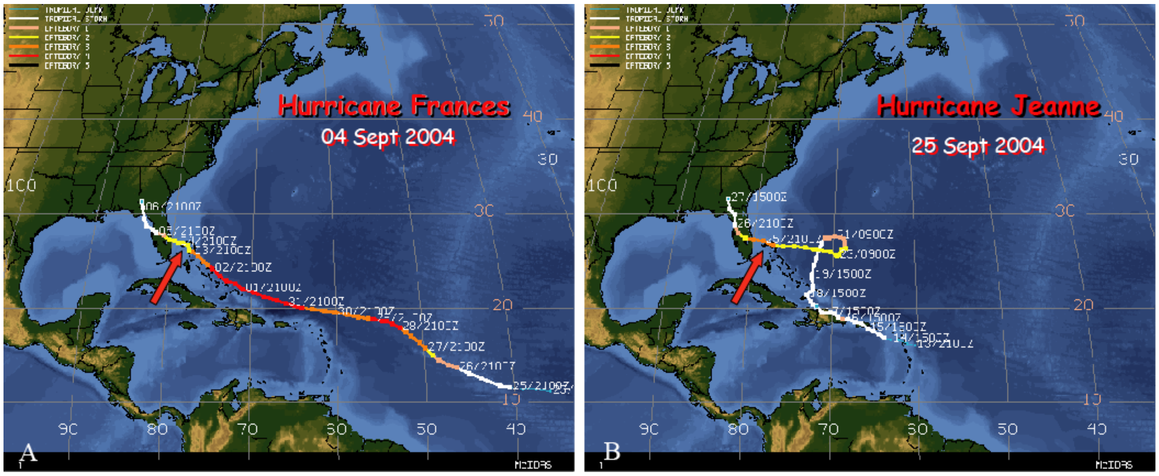

Figure 2: Hurricane tracks and intensity plots for Hurricanes Frances (A) and Jeanne (B) from September 2004. The red arrow indicates the location of the study area in the Northern Abacos, Bahamas. Figures are modified from the National Hurricane Center / Tropical Prediction Center's website (www.nhc.noaa.gov).

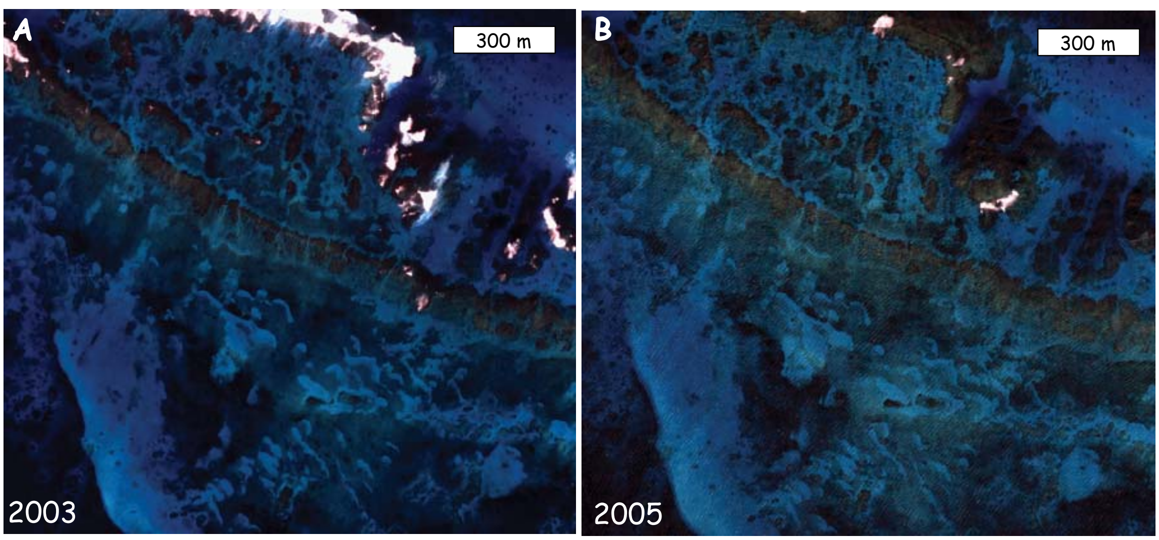

Figure 3: High-resolution remote sensing image of pre (A) and post (B) storm morphology of a portion of the barrier reef and its reef apron. This figure demonstrates the absence of significant geomorphic change (e.g., no expanded reef apron) during a period that included the passage of hurricanes Frances and Jeanne in 2004. Although there are some expanded sand patches around some patch reefs, no major geomorphic changes occur. (The whitish color on the pre-storm image in the yellow box are waves breaking on the reef crest, and the darker patches in the apron on the pre-storm image are most likely due to seasonal differences in sea-grass colonization rather than depth differences.) Image courtesy of DigitalGlobe.

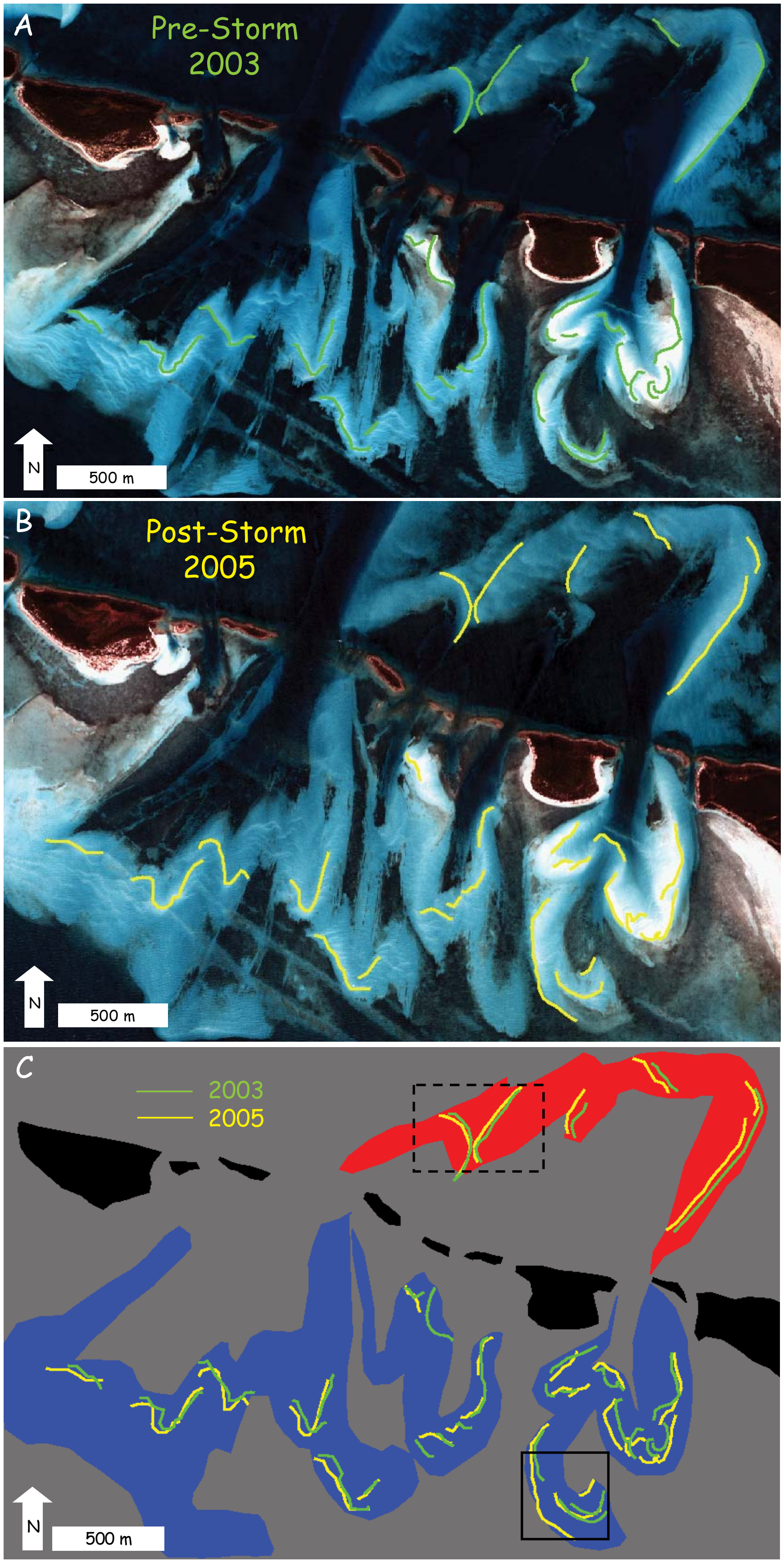
A
Pre-Storm
2003
N
500 m
B
Post-Storm
2005
N
500 m
C
2003
2005
N
500 m

Figure 4: Extent of the geomorphic changes that occurred over the 1.5-year period between remote sensing image acquisitions, during which the two storms (Hurricane Frances and Hurricane Jeanne) passed. The majority of the study area experienced few to no modifications, but the crests of some tidal deltas did move. This figure highlights key pre-storm crest locations (A, and green lines in C) and post-storm crest locations (B and yellow lines in C), selected to illustrate morphologic adjustments between the remote sensing images. The modifications are compared in C. Most of the crests on both flood and ebb deltas shifted to the southwest, but this is not the case for all the crests highlighted. See text for more details. Images copyright DigitalGlobe.

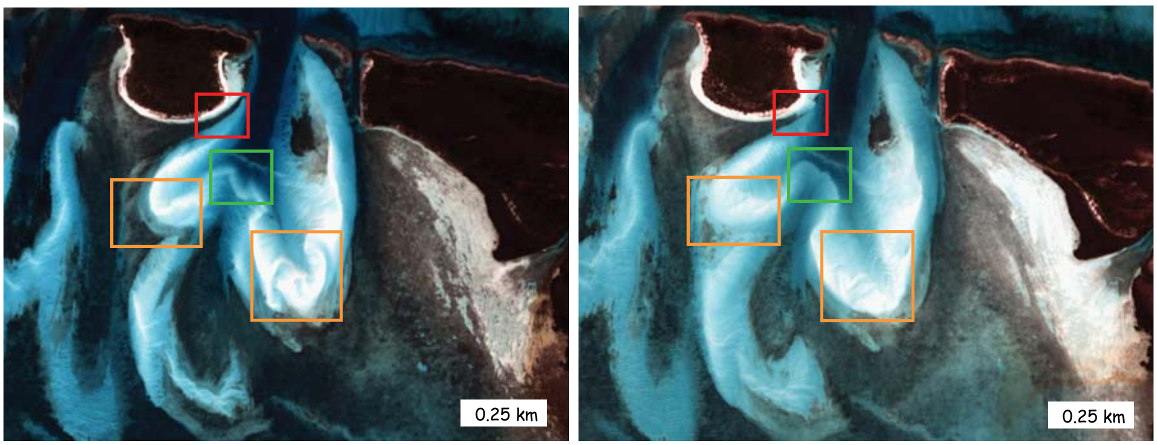

Figure 5: QuickBird high resolution remote sensing images of a flood lobe of a tidal delta near Carter's Cay, Bahamas, acquired in November, 2003 (A), and in March, 2005 (B). This time interval surrounds the active 2004 hurricane season that affected the regions, and shows one of the regions more affected by the storms, with erosion of seagrass (red box), migration of bar crests (green box) and sedimentation (orange boxes). Satellite image courtesy: DigitalGlobe.

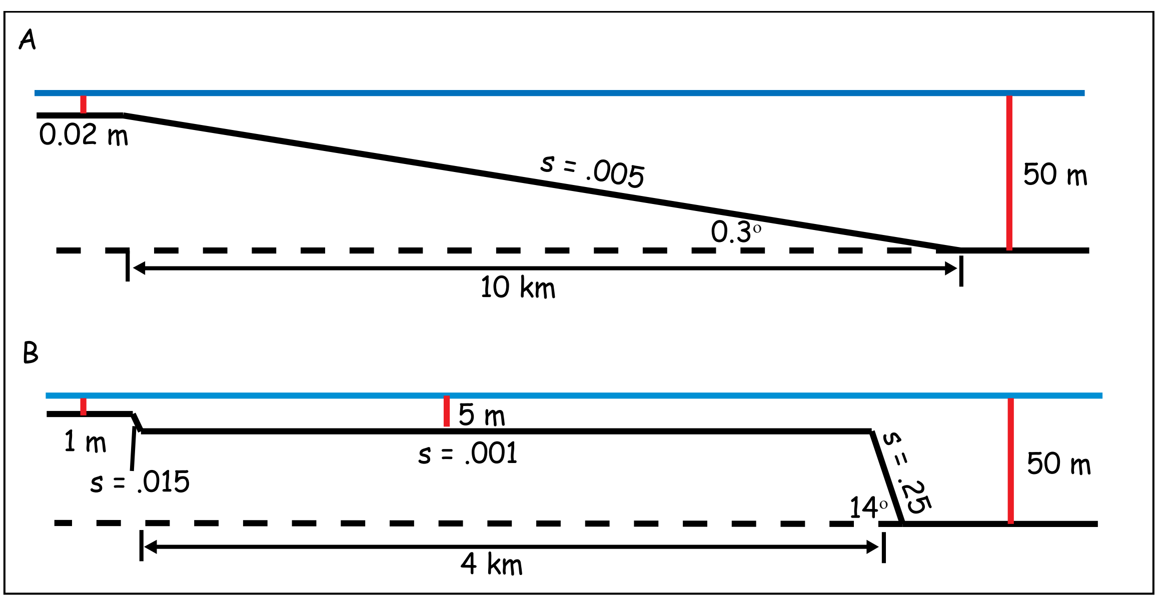

Figure 6: Bathymetric configurations for the ramp (A) and platform (B) situations modeled with the wave model. The platform bathymetry (B) consists of 3 different slopes used to determine the breaking criteria for the waves.

A

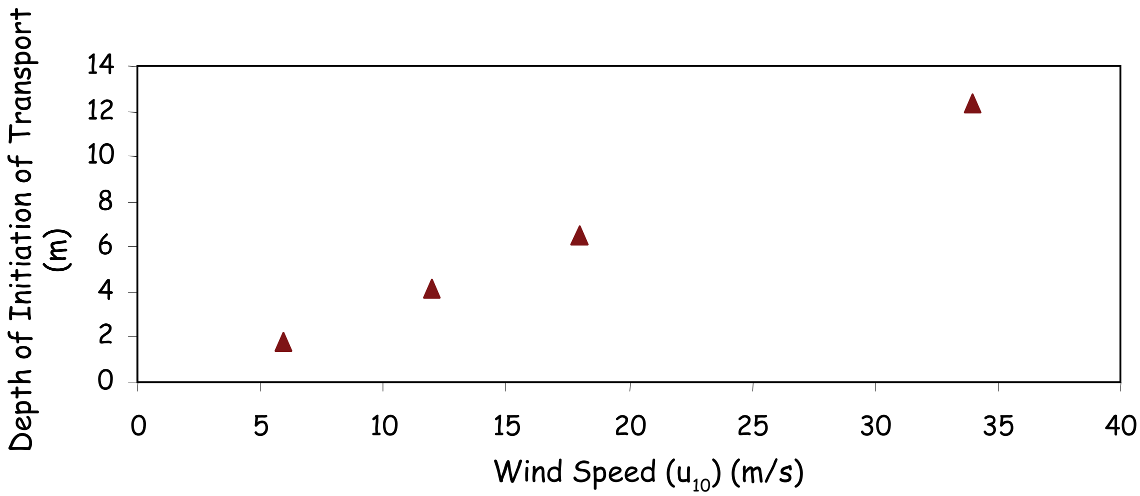

B

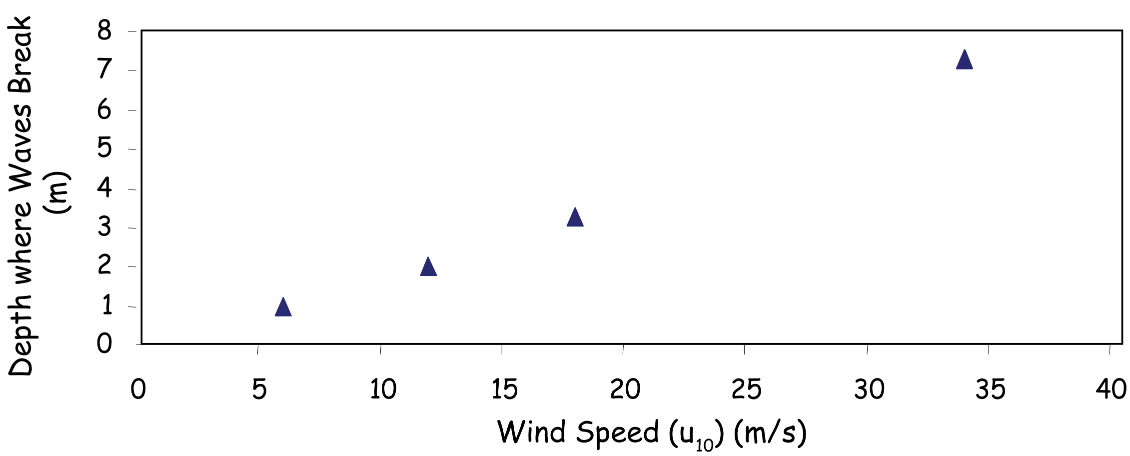

Figure 7: Wave model results for the simple ramp bathymetry at the peak frequency of the wave spectrum for 4 different wind speeds: daily 6.0 m/s winds, the average winter cold front winds (12 m/s), tropical storm winds (18 m/s), and Category 1 Hurricane strength winds (based on the Saffir-Simpson scale). A) This plot illustrates the depth at which the wave's bottom orbital velocity exceeds the threshold velocity of sediment entrainment. At depths shallower than these plotted values, bare sediment is being transported. Once a wave breaks, however, the energy disperses and the sediment transport is terminated (for that wave). The depths at which the waves break are shown in B. If the wave begins to transport sediment at 6.5 m water depth, but breaks in 4 m, it is only responsible for sediment transport along a short distance of the ramp.

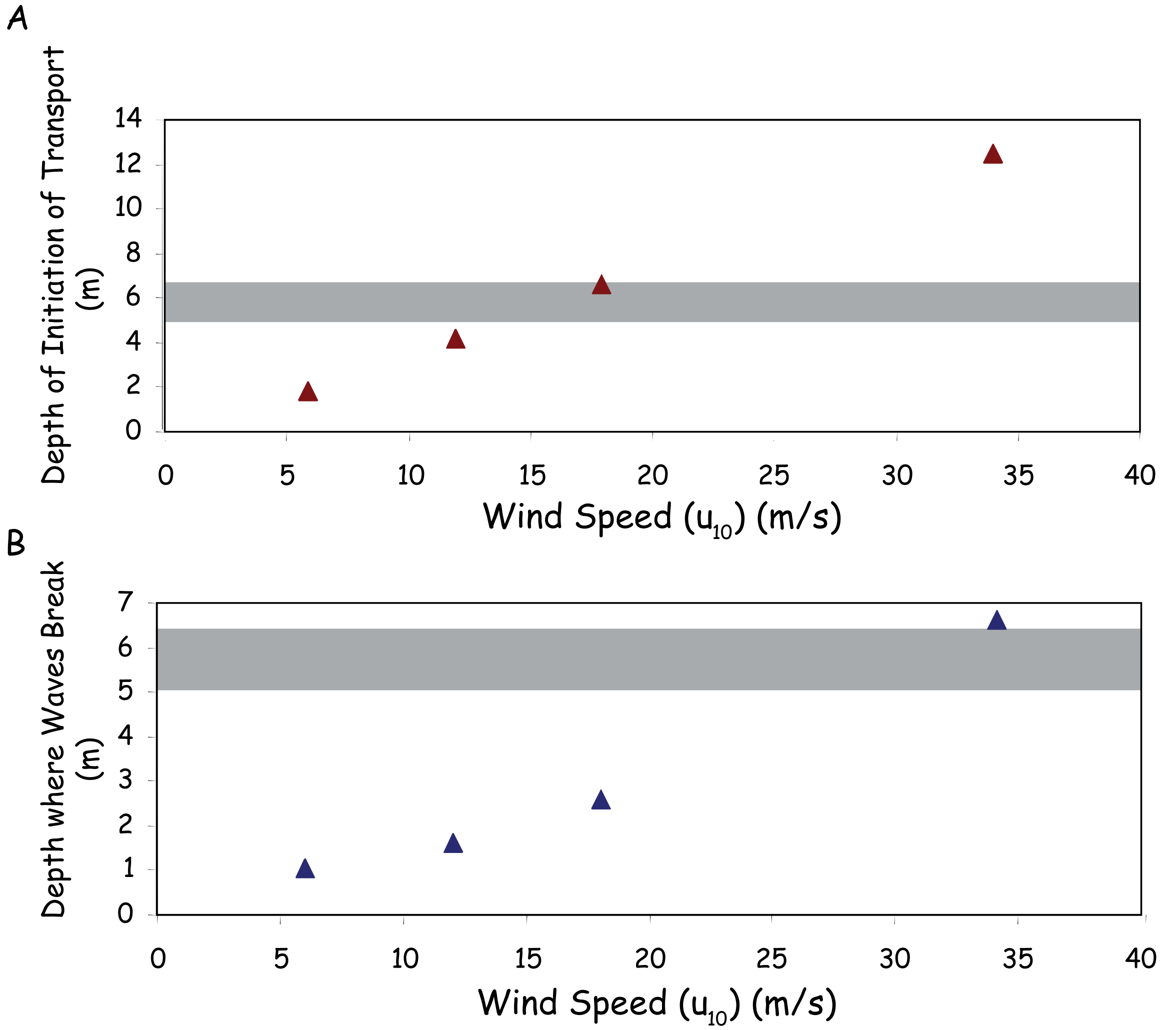

Figure 8: The results of the wave model for 5 frequencies under 4 different wind strengths (6 m/s, 12 m/s, 18 m/s (Tropical Storm), 34 m/s (Category 1 Hurricane)) over a shallow, unrimmed platform. Since the platform is flat and bottom friction is not accounted for, if the wave does not break on the reef, it will persist throughout the platform. This figure shows the depths at which each wave produced by the different wind conditions begins to move sediment at the bottom (A) and the depths at which the waves break and would therefore stop moving influencing the bottom. The gray box in both figures indicates the depth of the platform (which varies according to the storm surge). If the wave breaks above this gray box (B), the wave does not influence the platform. Similarly, if the depth of transport initiation is below this box (A), no sediment is transported on the platform. For model runs of storms of the order of Category 1 and greater, the waves break at the platform edge, so there is effectively less influence on the platform.

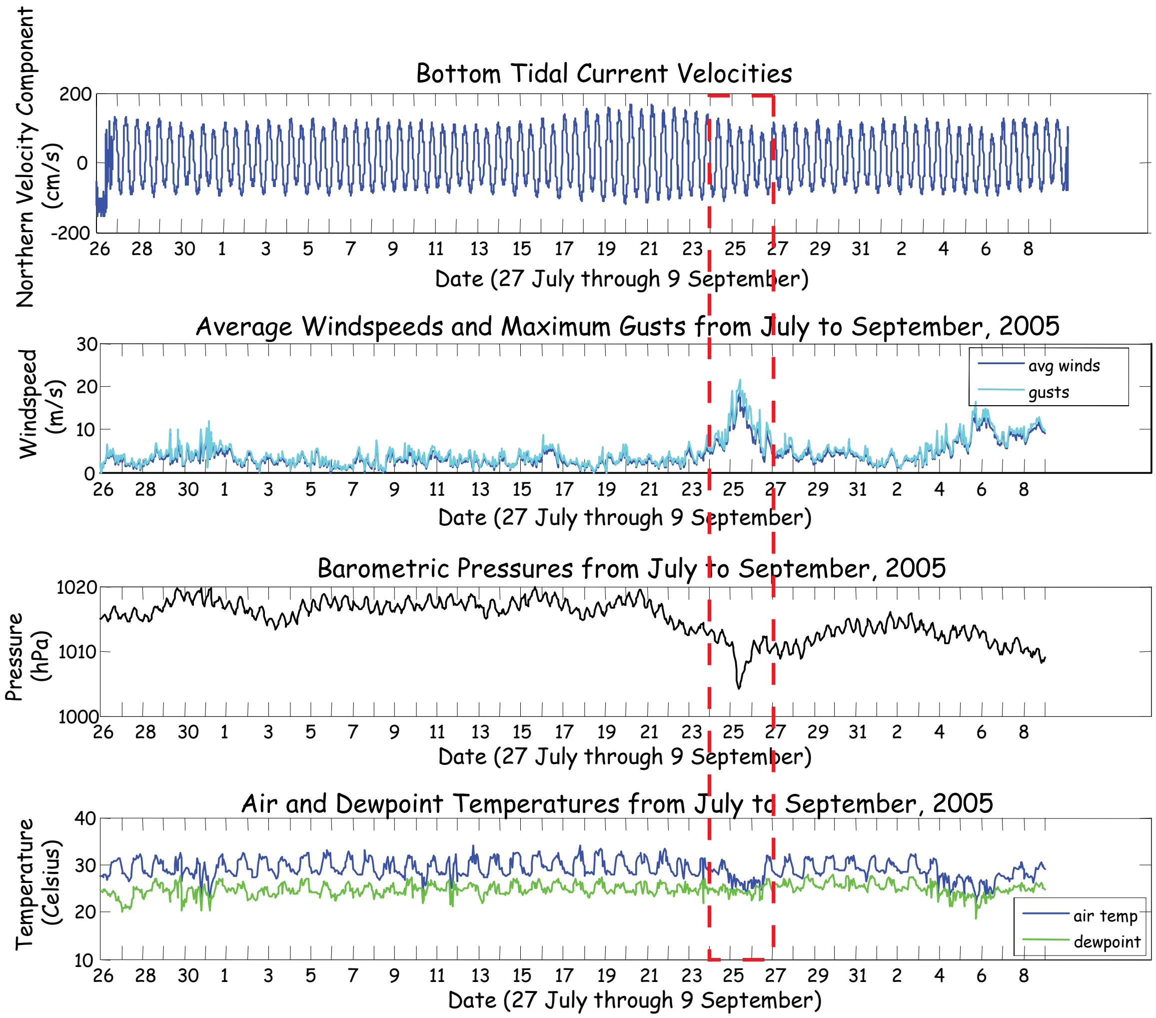

Figure 9: Comparison of the northern component of the tidal forcing at the bottom of a tidal delta (top) with atmospheric effects (NOAA buoy, bottom three plots) in late summer, 2005. The measurements were obtained by an ADCP located at ADCP1 in Figure 1. Although the presence of the storm (Hurricane Katrina, red dashed box) is obvious in the atmospheric data, it does not appear as obvious in the tidal measurements. Note that the average tidal velocities exceed 1 m/s, daily.

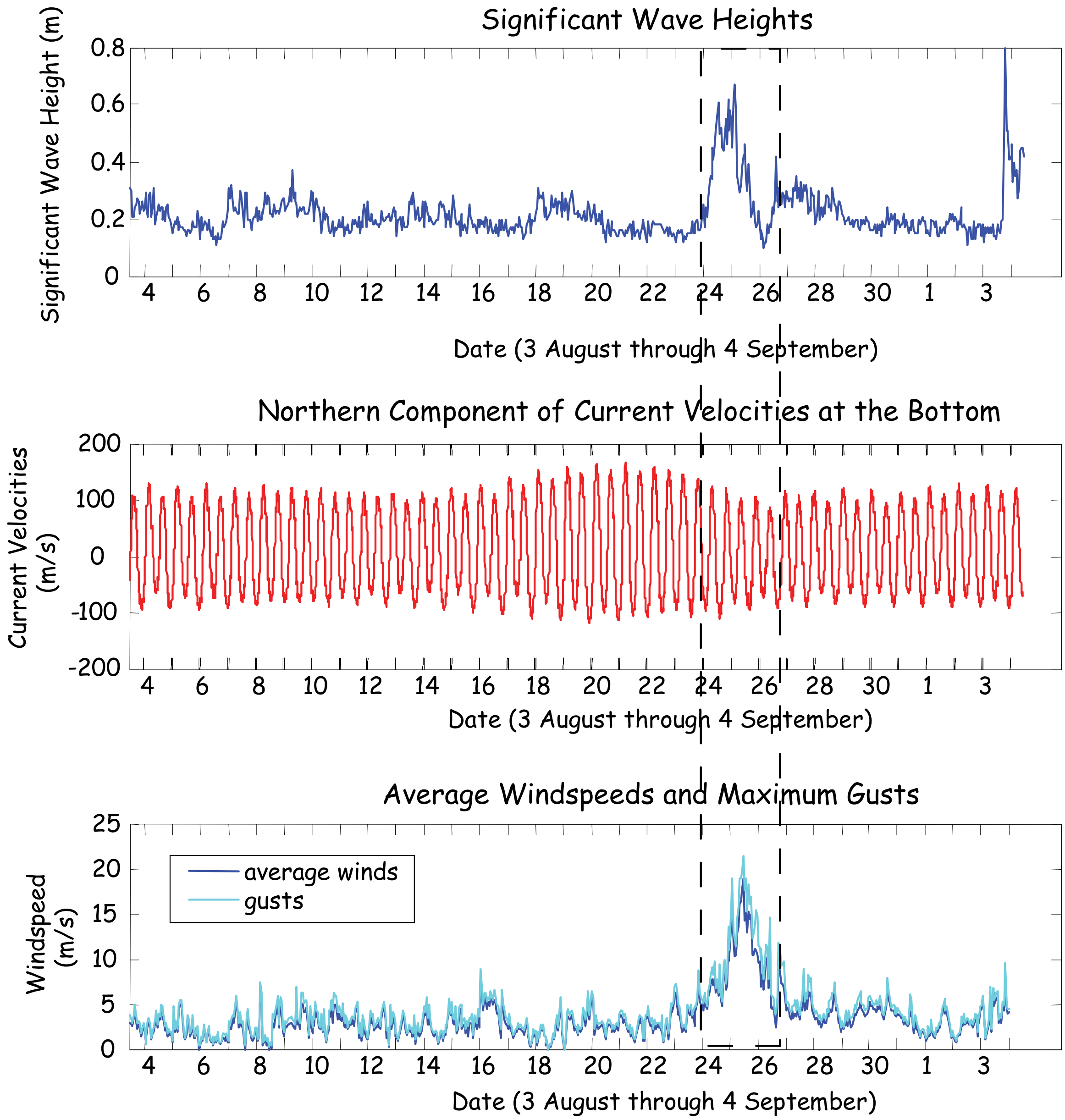

Figure 10: Wave gauge measurements (top) compared with the tidal velocities (middle) and atmospheric data from the NOAA buoy (bottom). The wave gauge was located between the reef and the apex of an ebb tidal delta (dark blue in Figure 1). The ADCP was located in the inlet between Jack's Cay and Carter's Cay (ADCP1 in Figure 1). The wave height increases in response to Hurricane Katrina (black dashed box) prior to the decrease in wind speeds. The waves in this region, however, generally remain between 0.2 and 0.4 m high.

U_{10} (m/s)	u_* (m/s)	H_0 (m)	T_p (s)	t_d (hr)
6	6.43	0.42	2.93	10.5
12	15.09	0.98	3.89	14.0
18	24.89	1.61	4.59	16.6
34	54.32	3.51	5.96	21.5

Table 2-1: Results of the deep water wave module computations. This table gives the values of the wind speed at 10 m above sea level (u_{10}), the wind stress factor (u_*), the deep water significant wave height (H_0), the peak period of the wave spectrum (T_p), and the time limit to the duration-limited sea state (t_d).

Category	Daily Winds	Storm Winds	Tropical Storm	Category 1
Wind speed	6 m/s	12 m/s	18 m/s	34 m/s
Surge	0.0 m	0.5 m	1.0 m	1.6 m

Table 2-2: Wind speed (u_{10}) and surge values used in the numerical wave model for the different types of winds: daily winds, storm winds (winter storm), and tropical cyclones of both Tropical Storm strength and Category 1 Hurricane strength (on the Saffir-Simpson Scale).

U_{10} (m/s)	H_0 (m)	T_p (s)	H_b (m)	h_b (m)	h_t (m)	u_{max} (m/s)
6	0.42	2.93	0.38	1.00	1.75	0.54
12	0.98	3.89	0.90	1.99	4.12	0.78
18	1.61	4.59	1.45	3.28	6.55	0.86
34	3.51	5.96	3.11	7.30	12.37	0.80

Table 2-3: Model results for the case of a gently-sloping carbonate ramp. H_b is the wave height when the wave breaks, h_b is the water depth at which the wave breaks, h_t is the depth where sediment begins to move ($u>u_t$), and u_{max} is the maximum orbital velocity obtained on the ramp prior to the wave breaking. See Table 2-1 for the other parameter definitions.

U_{10} (m/s)	H_b (m)	h_b (m)	h_t (m)	u_{max} (m/s)
6	0.38	1.01	1.75	0.53
12	0.93	1.57	4.11	1.03
18	1.49	2.58	6.50	1.17
34	3.12	6.60	12.35	0.99

Table 2-4: Results of the wave model for the simplified carbonate platform bathymetry. Refer to Table 2-3 for parameter definitions. If h_b > platform depth (5 m) + surge (refer to Table 2-2 for the surge value), the wave breaks before reaching the platform. If h_t < platform depth (5 m) + surge, the sediment on the platform top is not transported. The values for the platform differ from the results for the ramp (Table 2-3) due to the different bathymetries. Similarly, the different values in u_{max} within this table are due to the different bathymetrical gradients influencing the waves. Recall that u_{max} is the maximum orbital velocity obtained prior to breaking, not the orbital velocity produced on the flat platform.